

# Fabrication of $\text{Yb}^{3+}:\text{Er}^{3+}$ co-doped $\text{Al}_2\text{O}_3$ ridge waveguides by the dry etching

Qi Song,<sup>a</sup> Jin-Song Gao,<sup>a</sup> Xiao-Yi Wang,<sup>a</sup> Hong Chen,<sup>a</sup> Xuan-Ming Zheng,<sup>a</sup> Tong-Tong Wang,<sup>a</sup> Cheng-Ren Li,<sup>b</sup> and Chang-Lie Song<sup>b</sup>

<sup>a</sup>Changchun Institute of Optics, Optical Technology Center, Fine Mechanics and Physics, CAS, 130033, China

<sup>b</sup>Dalian University of Technology, Department of Physics, Dalian, 116024, China

**Abstract.** We present the fabrication process of straight-ridge  $\text{Yb}^{3+}:\text{Er}^{3+}$  co-doped  $\text{Al}_2\text{O}_3$  waveguides. Thin films are synthesized on silica-on-silicon wafers by middle frequency sputtering (MFS) and microwave ECR (MW-ECR) plasma source deposition. Waveguides are developed by reactive plasma etching employing  $\text{BCl}_3$  gas. Photoluminescence (PL) spectrum and gain measurements at  $1.53 \mu\text{m}$  are investigated at room temperature: a net gain of  $5.225 \text{ dB/cm}$  is achieved from a  $10.5\text{-mm}$ -long waveguide obtained by MFS, and  $0.043 \text{ dB/cm}$  is achieved from a MW-ECR with a  $980\text{-nm}$  pump power of  $62 \text{ mW}$ . © 2007 Society of Photo-Optical Instrumentation Engineers.  
[DOI: 10.1117/1.2721529]

Subject terms: erbium; optical amplifiers; dry etching; optical gain.

Paper 060612LR received Aug. 12, 2006; revised manuscript received Jan. 30, 2007; accepted for publication Jan. 31, 2007; published online Apr. 5, 2007.

Erbium-doped waveguides have demonstrated strong potential<sup>1,2</sup> in optical communication as a typical active optical device that could provide optical gain at  $1.53 \mu\text{m}$  via energy level transition  $^4\text{I}_{13/2} \rightarrow ^4\text{I}_{15/2}$ . The luminescence emission of  $\text{Er}^{3+}$ -doped devices can be improved in silica fiber and other hosts by co-doping with  $\text{Yb}^{3+}$  ions, which act as sensitizers of the  $\text{Er}^{3+}$  luminescence, with a broader and more intense excitation band available to semiconductor laser excitation.

Due to notable advantages such as high thermal conductivity, excellent mechanical properties, moderate maximum phonon energy, and high solubility of erbium in the  $\text{Al}_2\text{O}_3$  matrix,  $\text{Al}_2\text{O}_3$  was generally investigated as one of the promising waveguide materials.<sup>3-5</sup> In our previous work, middle frequency sputtering (MFS) and microwave ECR (MW-ECR) plasma source deposition were studied and reported to be more efficient methods to obtain high quality  $\text{Al}_2\text{O}_3$  thin films.<sup>6,7</sup> In this letter, we present the fabrication processes of straight rib-channel  $\text{Yb}^{3+}:\text{Er}^{3+}$  co-doped  $\text{Al}_2\text{O}_3$  waveguides.  $\text{Yb}^{3+}:\text{Er}^{3+}$  co-doped  $\text{Al}_2\text{O}_3$  thin films were deposited by MFS and MW-ECR plasma source deposition. Thin films were etched by a reactive plasma etching technique employing  $\text{BCl}_3$  gas. The photoluminescence (PL) spectrum of thin films and the optical gain of waveguide chips at  $1.53 \mu\text{m}$  were investigated at room temperature. A net gain of  $5.225 \text{ dB/cm}$  was achieved from a  $10.5\text{-mm}$ -long waveguide obtained by MFS, and

$0.043 \text{ dB/cm}$  was achieved from a MW-ECR with a  $980\text{-nm}$  pump power of  $62 \text{ mW}$ .

Experimentally, thin films are deposited on silica-on-silicon wafers that were oxygenated for a  $0.3\text{-}\mu\text{m}$   $\text{SiO}_2$  layer. The Er and Yb metal bulks are embedded in the Al target. The Er content is measured to be constant as  $1.8\%$  after deposition, and Yb content was changed by increasing the number of Yb bulks in the Al target. For both fabrication processes, the samples are deposited for 2 h and annealed in air. We found that further deposition beyond 2 h in the MFS system deteriorates the surface of thin films, and the deposition rate of thin films decreases, which causes the PL intensity to increase slightly. The experiment setups and parameters related to the fabrication process are shown in detail in our previous work.<sup>7</sup>

The SEM schematics of the surface and cross-section of thin films prepared by MFS and MW-ECR are shown in Fig. 1. For the MFS samples,  $0.9$  to  $1.1 \mu\text{m}$   $\text{Al}_2\text{O}_3$  layers and small defects on the surface are produced by intense discharge. However, there are no defects on the surface of thin films formed by MW-ECR with a steady and strong plasma source,<sup>7</sup> and the thickness of the 2-h deposition is about  $0.5 \mu\text{m}$ .

Due to the defects on the surface of the MFS sample, the  $100\text{-nm}$   $\text{SiO}_2$  layer was deposited on the  $\text{Al}_2\text{O}_3$  layer to reduce the influence of defects on the surface. The reactive plasma etching process is illustrated in Figs. 2(a)–2(c): A photoactive layer was formed by the spin-on technique and roasted on the surface of the  $\text{Al}_2\text{O}_3$  thin films. A patterned mask was placed on the photoactive layer, and an ultraviolet beam was projected incident on the mask to remove the exposure part. The positive pattern was formed on the top of layer. A thin film was then placed into the reactive chamber, and rf voltage was applied on the substrate. The  $\text{BCl}_3$  plasma flow was induced onto the surface to uncover the  $\text{Al}_2\text{O}_3$  layer. The  $\text{Al}_2\text{O}_3$  layer was patterned through the mask with five straight channels, leading to ridges  $3.2$  to  $4 \mu\text{m}$  wide, separated from one another by  $50 \mu\text{m}$ . The etching depth is controlled by the concentration of etching gas and reactive time. The etching area is  $10.5 \text{ mm} \times 9 \text{ mm}$ . Since the photoactive material is composed of hydrocarbon,  $\text{O}_2$  flow was induced to remove the photoactive lines. After etching, the  $\text{SiO}_2$  layer on the waveguide lines was eliminated by hf.

The waveguides are investigated by electron microprobe analysis (EMPA). Figure 2(d) shows the schematic diagrams of the  $\text{Yb}^{3+}:\text{Er}^{3+}$  co-doped  $\text{Al}_2\text{O}_3$  rib-channel waveguides. The sidewall of the waveguide is irregular because of the anisotropy of reactive  $\text{BCl}_3$  plasmas, which may lead to the energy leak and the increase of optical loss. The rib-channel depth of the  $\text{Al}_2\text{O}_3$  layer deposited by MFS is about  $0.7$  to  $0.8 \mu\text{m}$ , and the rib-channel depth of the  $\text{Al}_2\text{O}_3$  layer deposited by MW-ECR is about  $0.5$  to  $0.6 \mu\text{m}$ .

In the PL/gain measurement system, a  $980\text{-nm}$  LD and a  $1530\text{-nm}$  LED are coupled into a Y coupler and focused to a cross section of the waveguide from a tapered single-mode optical fiber, located by an optical fiber adjuster. For gain measurement, the LED signal is modulated with a  $160\text{-Hz}$  frequency generator and collected by an InGaAs detector. The amplified signal is demodulated using the lock-in technique to remove spontaneous emission noise. Figure 3 shows the PL spectrums of the  $\text{Yb}^{3+}:\text{Er}^{3+}$  co-

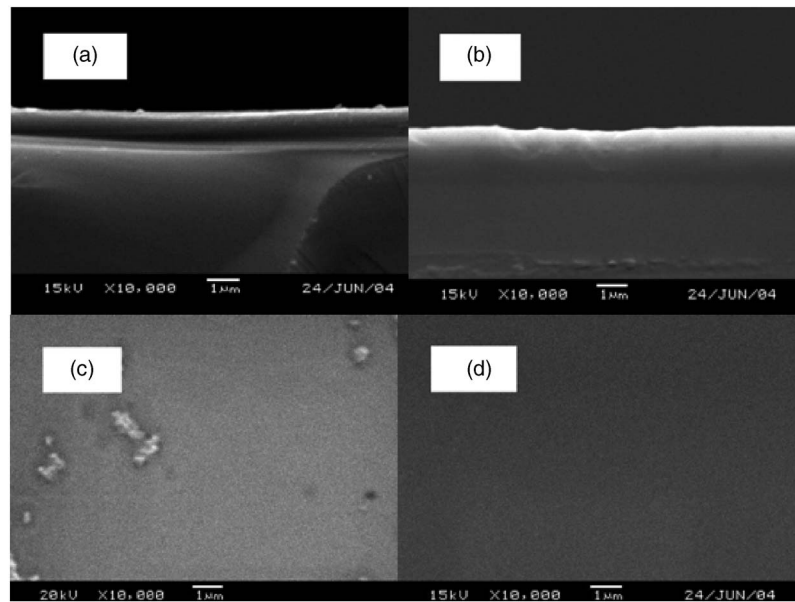


**Fig. 1** Schematics of the cross section and surface of  $\text{Yb}^{3+}:\text{Er}^{3+}$  co-doped  $\text{Al}_2\text{O}_3$  thin films prepared by MW-ECR and MFS. For the MFS samples shown in (a) and (c), the  $\text{Al}_2\text{O}_3$  layer is about 1.2 to 1.4  $\mu\text{m}$ , and small defects on the surface are formed during the deposition. For the MW-ECR samples shown in (b) and (d), no defects are formed on the surface, and the thickness of the 2-h deposition is about 0.7 to 1  $\mu\text{m}$ .

doped  $\text{Al}_2\text{O}_3$  waveguides prepared by MFS and MW-ECR, pumped at 2000 mA by 980 nm at room temperature. Curve *a* represents the PL spectrum of the MFS sample, with an optimal  $\text{Yb}^{3+}:\text{Er}^{3+}$  ratio of 6:1, annealed at 850 °C;

Curve *b* represents the PL spectrum of the MW-ECR sample, with an optimal  $\text{Yb}^{3+}:\text{Er}^{3+}$  ratio of 3.6:1, annealed at 900 °C. The PL peak intensity of the MFS sample is 5 times higher than that of the MW-ECR sample.

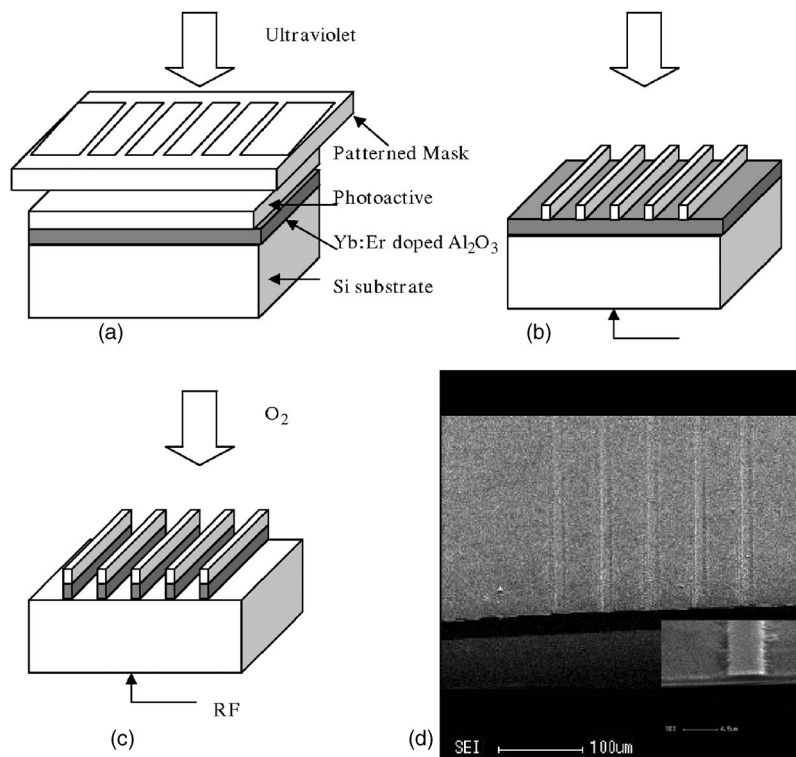


**Fig. 2** (a) to (c) Diagrams of the reactive plasma etching process of the  $\text{Al}_2\text{O}_3$  waveguide. (d) Schematics of the  $\text{Yb}^{3+}:\text{Er}^{3+}$  co-doped  $\text{Al}_2\text{O}_3$  waveguides prepared by MFS and MW-ECR and etched by plasma dry etching employing  $\text{BCl}_3$  gas. The rib width is 4  $\mu\text{m}$ , and the interval between the channels is 50  $\mu\text{m}$ . The waveguide chip area is 10.5 mm  $\times$  10 mm.

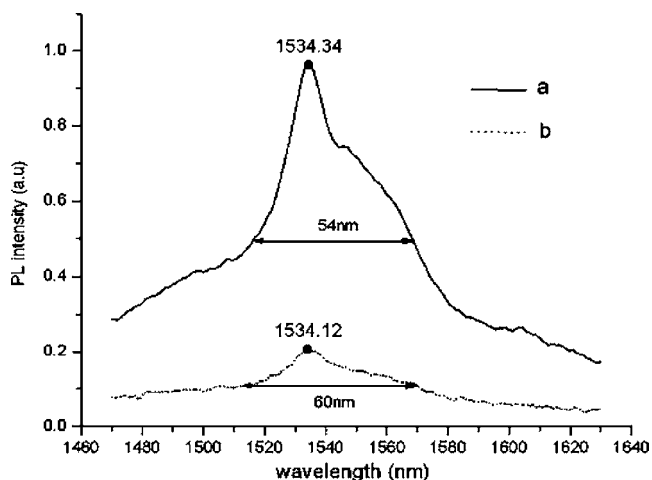


**Fig. 3** PL spectrums of the MFS and MW-ECR samples at  $1.53 \mu\text{m}$ . Curve *a* represents the PL spectrum of the MFS sample, with a  $\text{Yb}^{3+}:\text{Er}^{3+}$  ratio of 9:1, annealed at  $850^\circ\text{C}$ . Curve *b* represents the PL spectrum of the MW-ECR sample, with a  $\text{Yb}^{3+}:\text{Er}^{3+}$  ratio of 5:1, annealed at  $900^\circ\text{C}$ . The optimal PL intensity of the MFS sample is 5 times higher than that of the MW-ECR sample.

In Fig. 4, curve *a* is the gain curve of the waveguide chip prepared by MFS; curve *b* is the gain curve of the waveguide chip prepared by MW-ECR. The net gain curves are deduced from the direct ratio of output and input signal intensity in the system, which includes the coherent loss of the coupling, internal absorbing, and transmitting in the waveguides. As the pump power increases to 62 mW, the net gain of curve *a* and curve *b* increases to 5.486 dB and 0.045 dB at a length of 10.5 mm. The threshold of curve *a*

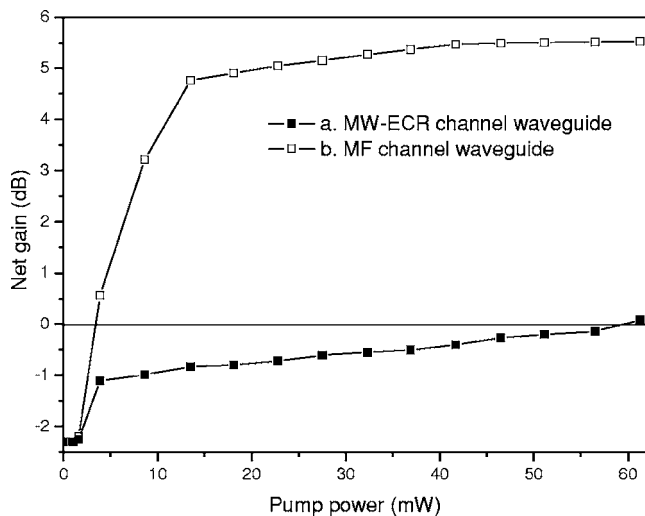


**Fig. 4** Dependence of the pump power and gain of the waveguide.

is 3.33 mW, and the gain saturates under a pump power of 13.5 mW; the threshold of curve *b* is 60 mW, and the gain saturates under 4 mW. As a result of short waveguide length, the gain curves of the waveguides are saturated at a very low pump power.

With the same signal and pump powers, the signal net gain of the waveguide prepared by MFS is higher than that prepared by MW-ECR. This may be because the discrepancy of the thickness of the waveguides allows more pump-wave modes to exist in the waveguides, and more pump power can be coupled into the waveguides. Another essential aspect is that more active Er ions in the MFS waveguide are present than in the MW-ECR waveguide.<sup>8</sup> The coherent effects were also demonstrated in the PL spectrum.

In summary, the fabrication process of straight-ridge  $\text{Yb}^{3+}:\text{Er}^{3+}$  co-doped  $\text{Al}_2\text{O}_3$  waveguides is introduced based on MFS and MW-ECR plasma deposition. The PL spectrum of thin films and gain curves of the rib-channel waveguide are measured at room temperature. Net gains of 5.486 dB and 0.045 dB were obtained from 10.5-mm-long waveguide chips prepared by MFS and MW-ECR under 62-mW pump power. This method is promising for obtaining larger net gains at longer lengths and can be applied to construct optical amplifiers for metropolitan applications in an in-line configuration without the requirement of a folded channel.

#### Acknowledgments

The authors would like to thank Xin-Lu Deng, Guo-Qing Li, Jun Xun, and Wan-Yu Ding for the thin film fabrication and Jie-Ping Han for the etching technique. This work was partly supported by the NNSFC (Grant Nos. 69889701 and 60478035).

#### References

1. A. Polman, J. S. Custer, E. Snoeks, and G. N. van den Hoven, "Incorporation of high concentrations of erbium in crystal silicon," *Appl. Phys. Lett.* **62**, 507 (1993).
2. A. Polman, "Exciting erbium-doped planar amplifier materials," in *Proc. Photonic West Conference Proc. SPIE* **3942**, 2 (2000).
3. C. Strohhofer and A. Polman, "Relationship between gain and Yb concentration in Er-Yb doped waveguide amplifiers," *J. Appl. Phys.* **90**, 4314 (2001).
4. C. Strohhofer and A. Polman, "Absorption and emission spectroscopy in  $\text{Er}^{3+}$ - $\text{Yb}^{3+}$  doped aluminum oxide waveguides," *Opt. Mater. (Amsterdam, Neth.)* **21**, 705 (2003).
5. Y. C. Yan, A. J. Faber, and H. de Waal, "Erbium-doped phosphate glass waveguide on silicon with 4.1 dB/cm gain at 1535 nm," *Appl. Phys. Lett.* **71**, 17 (1997).
6. J. Xu, X. L. Deng, J. L. Zhang, W. Q. Lu, and T. C. Ma, "Characterization of CN films prepared by ECR plasma source enhanced DC magnetron sputtering," *Thin Solid Films* **390**, 107–112 (2001).
7. Q. Song, C. R. Li, and J. Y. Li, "Photoluminescence properties of the Yb:Er co-doped  $\text{Al}_2\text{O}_3$  thin film fabricated by microwave ECR plasma source enhanced RF magnetron sputtering," *Opt. Mater. (Amsterdam, Neth.)* **28**(12), 1344–1349 (2006).
8. Q. Song, C.-R. Li, and J.-Y. Li, "Effect of pulse  $\text{CO}_2$  laser annealing on the crystallization of  $\text{Yb}^{3+}:\text{Er}^{3+}$  co-doped  $\text{Al}_2\text{O}_3$  thin film to a silica-on-silicon substrate," *Opt. Commun.* available online (2006).